International Journal of Pharmaceutics 512 (2016) 22–31

Contents lists available at ScienceDirect

International Journal of Pharmaceutics

journal homepage: www.elsevier.com/locate/ijpharm

(−)-Epigallocatechin gallate (EGCG)-nanoethosomes as a transdermal delivery system for docetaxel to treat implanted human melanoma cell tumors in mice

Bingwu Liao[a,1], Hao Ying[a,1], Chenhuan Yu[b,1], Zhaoyang Fan[a], Weihua Zhang[a], John Shi[c], Huazhong Ying[b], Nagaiya Ravichandran[a], Yongquan Xu[d], Junfeng Yin[d], Yongwen Jiang[d], Qizhen Du[a,*]

[a] The Key Laboratory for Quality Improvement of Agricultural Products of Zhejiang Province, The College of Agricultural and Food Sciences, Zhejiang A & F University, Linan 311300, China
[b] Experimental Animal Center of the Zhejiang Academy of Medical Sciences, Hangzhou 310013, China
[c] Guelph Food Research Center, Agriculture and Agri-Food Canada, Guelph, Ontario N1G 5C9, Canada
[d] Tea Research Institute, Chinese Academy of Agricultural Sciences, Key Laboratory of Tea Biology and Resources Utilization, Ministry of Agriculture, Hangzhou 310008, China

ARTICLE INFO

Article history:
Received 12 May 2016
Received in revised form 31 July 2016
Accepted 17 August 2016
Available online 18 August 2016

Chemical compounds studied in this article:
(−)-Epigallocatechin-3-*O*-gallate (PubChem CID: 65064)
Docetaxel (PubChem CID: 148124)

Keywords:
(−)-Epigallocatechin-3-*O*-gallate
Nanoethosomes
Transdermal delivery
Docetaxel
Skin cancer
Pharmacokinetics

ABSTRACT

(−)-Epigallocatechin-3-*O*-gallate (EGCG), a versatile natural product in fresh tea leaves and green tea, has been investigated as a preventative treatment for cancers and cardiovascular disease. The objective of this study was to develop EGCG-nanoethosomes for transdermal delivery and to evaluate them for treating subcutaneously implanted human melanoma cell tumors. EGCG-nanoethosomes, composed of 0.2% EGCG, 2% soybean phosphatidylcholine, 30% ethanol, 1% Tween-80 and 0.1% sugar esters, were prepared and characterized using laser transmission electron microscopy. These nanoethosomes were smoother and more compact than basic-nanoethosomes with the same components except for EGCG. The effectiveness of transdermal delivery by EGCG-nanoethosomes was demonstrated in an *in vitro* permeability assay system using mouse skin. The inhibitory effect of docetaxel (DT) loaded in EGCG-nanoethosomes (DT-EGCG-nanoethosomes) was analyzed by monitoring growth of a subcutaneously implanted tumor from A-375 human melanoma cells in mice. Mice treated with DT-EGCG-nanoethosomes exhibited a significant therapeutic effect, with tumors shrinking, on average, by 31.5% of initial volumes after 14 d treatment. This indicated a potential for treating skin cancer. In a pharmacokinetic study, transdermal delivery by DT-EGCG-nanoethosomes enabled sufficient DT exposure to the tumor. Together, these findings indicated that EGCG-nanoethosomes have great potential as drug carriers for transdermal delivery.

1. Introduction

Nanoethosomes promote high bioavailability by carrying substances through the skin more effectively than either conventional liposomes or hydroalcoholic solutions (Touitou and Godin, 2007; Elsayed et al., 2006). Nanoethosomes, with synergistic actions of ethanol, vesicles and skin lipids, can enhance delivery of active agents (Touitou et al., 2000; Touitou et al., 2001; Dubey et al., 2007a,b; Zhang et al., 2012). Nanoethosomes penetrate primarily through the pilosebaceous unit and partly through intercellular spaces (Xing et al., 2011). Their use can increase the residence time of drugs or cosmetic chemicals in the stratum corneum and epidermis and reduce systemic absorption of these agents. Their properties allow nanoethosomes to penetrate easily into the deeper layers of the skin and circulation (Verma and Pathak, 2010). To date, nanoethosomes have not been extensively

* Corresponding author.
E-mail address: qizhendu@163.com (Q. Du).
[1] These authors contributed equally.

http://dx.doi.org/10.1016/j.ijpharm.2016.08.038
0378-5173/

adopted into practice because of their ineffective improvement of transdermal permeability or low stability of nonotheosome suspensions. However, nanoethosomes, when optimized for composition and size, are a potentially promising means for not only cosmeceutical applications, but also for topical, noninvasive pharmaceutical treatment of local and systemic disorders (Chandel et al., 2012).

(−)-Epigallocatechin gallate (EGCG) has antioxidant activity about 25–100 times more potent than vitamins C or E (Zaveri, 2006) and has shown substantial benefits for treating various chronic disorders such as cancers, cardiovascular disease and obesity (Singh et al., 2011; Yang et al., 2009; Widlansky et al., 2007). However, EGCG has low bioavailability (Li et al., 2013; Sang et al., 2005; Krook and Hagerman, 2012). In humans, the oral bioavailability of EGCG by drinking tea, containing catechins at 10 mg/kg body weight, is about 0.1% (Warden et al., 2001; Lambert et al., 2006; Lee et al., 2014). This low bioavailability is partly because of the low stability of ECCG in bodily fluids (Wang et al., 2008). In our preliminary experiments to improve stability of EGCG with nanoethosomes, we found that EGCG-nanoethosomes were more stable than those made without EGCG. This finding encouraged us to investigate the loading of drugs into EGCG-nanoethosomes for transdermal delivery.

Skin cancers are by far the most common malignancy in humans, particularly in the white population, with over a million cases detected each year (D'Orazio et al., 2013). Malignant melanoma of the skin (MMS) is the deadliest form of skin cancer. MMS is often a treatment-refractory and metastasis-prone malignancy and its incidence has increased gradually, but significantly, over the last several decades (Narayanan et al., 2010). MMS are invasive and rapidly metastasize, making long-term survival poor for patients with advanced disease. It was estimated that 132,000 new cases of melanoma occur worldwide each year. According to an estimate from the World Health Organization, as many as 65,000 die per year, worldwide, from malignant skin cancer (WHO, 2011).

Recently, it has become increasingly clear that development of new drugs is not alone sufficient to increase therapeutic progress. Promising findings obtained *in vitro* are very often followed by less compelling results *in vivo*. One strategy to address this problem would be development of suitable drug carrier systems, such as nano-formulations of drugs, enabling localized and controlled drug release (Simoes et al., 2015). Docetaxel (DT) is a clinically well-established anti-mitotic chemotherapy medication that interferes with cell division. DT was approved by the FDA for treatment of several cancers (Clarke and Rivory, 1999). In our study, DT was loaded into EGCG-nanoethosomes to improve its bioavailability, *via* transdermal delivery, for treating skin tumors.

2. Experimental procedures

2.1. Materials

EGCG with a purity of 98% was provided by the Tea Research Institute of the Chinese Academy of Agricultural Sciences, Hangzhou, China. Docetaxel (DT) and Tween-80 were from Sigma-Aldrich (Shanghai, China). Soybean phosphatidylcholine lipid S100 (SPC) was from Shanghai Toshisun Biology & Technology Co., Ltd. (Shanghai, China). Sucrose esters were from Hangzhou Jinhelai Food Additives Co. Ltd. (Hangzhou, China).

2.2. Preparation of nanoethosomes

Nanoethosomes were prepared by a previously reported method with some modifications (Touitou et al., 2000). SPC, Tween-80 and sucrose esters were dissolved in ethanol in a glass bottle. The bottle was sealed and connected to a syringe pump with Teflon tubing. The solution, at room temperature, was stirred using a magnetic stirrer at 1000 rpm and Milli-Q water added at a constant rate of 1 ml/min through a syringe pump. The mixtures were treated with an ultrasonic processor (FS-1800N, Shanghai Sonxi Ultrasonic Instrument Company, Shanghai, China) 5 times, with a 5-s ultrasonication pulse each. Optimization of nanoethosomes was achieved by varying percentages of SPC, ethanol, Tween-80, EGCG and sucrose esters from 1 to 4%, 10 to 40%, 0 to 2.0%, 0 to 0.25% and 0 to 0.20%, respectively.

Nanoethosomes with DT were prepared using the same method and optimal amounts of SPC 2%, ethanol 30%, Tween-80 1%, EGCG 0.2% and sucrose esters 0.1%. EGCG and DT were dissolved in ethanol prior to mixing with SPC.

2.3. Characterization of nanoethosomes

The size distribution of nanoethosomes was analyzed using zeta potential measurements (Zetasizer ZS 90, Malvern Instruments, Malvern, UK). The morphology and size of the nanoethosomes were assessed using transmission electron microscopy (JEOL, JEM 2010F). The dispersion of nanoethosomes diluted with pure water was adsorbed onto carbon-coated formvar film that was attached to a metal specimen grid. Excess sample was removed by blotting and the grid was covered with a small drop of staining solution (2% w/v uranyl acetate). The staining solution was left on the grid for a few minutes and then excess solution drained. The sample was allowed to dry thoroughly in air and then examined under a transmission electron microscope (Madheswaran et al., 2014).

2.4. Entrapment efficiency and stability

To confirm stability of EGCG-nanoethosomes, the formulations were kept in sealed amber colored glass vials and stored at 2–8 °C or 25 °C. The particle size, polydispersity index (PI), zeta potential (ZP) and entrapment efficiency (EE) of these formulations were measured at predetermined time intervals and compared with values obtained with the fresh formulations (Hong et al., 2014). Furthermore, EGCG release studies were performed comparing values for formulations stored at 25 °C for 3 months with those for fresh formulations. A suspension of EGCG-nanoethosomes (2 ml) was placed in an Amicon Ultra-3K centrifugal filter device (Millipore Corp., Billerica, MA, USA) composed of a centrifuge tube and filter unit with a low-binding Ultracel membrane (3000 MWCO). After centrifugation at $4000 \times g$ for 3 min, free EGCG crossed the Ultracel membrane and could be recovered in the solution in the centrifuge tube. The EGCG incorporated into the EGCG-nanoethosomes was calculated based on the concentration of free EGCG. The EGCG concentration of the solution was determined by high-performance liquid chromatography (HPLC). The HPLC analysis was performed on a Shimadzu HPLC system (Shimadzu, Kyoto, Japan) with two LC-10A pumps, an SIL-10Avp autosampler, an SPD-M10Avp UV detector and a Symmetry C18 (5 m, 4.6 mm × 250 mm) column. The elution employed a linear gradient system using mobile phase A (water/acetic acid 98:2) and mobile phase B (acetonitrile) at a flow rate of 1 ml/min at 40 °C. The chromatogram was recorded by uv absorbance at 280 nm. The EE (%) of EGCG in the nanoethosomes and the loading amount (mg/g) were calculated from the results of HPLC analysis.

EE (%) = 100 × (total EGCG in nanoethosome suspension − free EGCG)/total EGCG in nanoethosome suspension

2.5. Determination of the transdermal permeability of nanoethosomes in vitro

The skin penetration depth of the nanoethosomes was determined with rhodamine red as a tracer using the method reported by Touitou et al. (2000). Rhodamine red-nanoethosome dispersions (250 μl) were applied non-occlusively to the surface of skin harvested from mice (HRS/J hairless mice, 6 w old) in a Franz diffusion cell and samples were incubated at 37 °C for 4 h. After incubation, the skin was removed and washed with 37 °C distilled water. Skin specimens were analyzed by confocal laser scanning microscopy at 10-μm increments through the z-axis and sequential images were collected on slide film. The fluorescence intensity was analyzed using a Sarastro Phoibos 1000 confocal laser scanning microscope (Molecular Dynamics, Sunnyvale, CA, USA) attached to a universal Zeiss epifluorescence microscope with an oil-immersed Plan apo 63 × 1.4 NA objective lens (Zeiss, Oberkochen, Germany). Optical excitation was administered with a 488-nm argon laser beam and fluorescence emission was detected above 560 nm. Samples were observed through the z-axis.

2.6. In vitro *permeation and skin deposition studies of DT released by DT-EGCG-nanoethosomes*

Skin from hairless mice (HRS/J), including epidermis and dermis, was harvested from the abdomen after sacrificing the animals. Skin samples were washed with normal saline and dried between two filter papers. Skin samples were used immediately, without storage.

Experiments were conducted in Franz diffusion cells having a receptor compartment volume of 6.5 ml. The *in vitro* study design was similar to that described by Elsayed et al. (2006). Isotonic phosphate buffer (pH 7.4) containing 0.11% (w/v) formaldehyde was used as the receptor medium. Skin membranes were mounted with the stratum corneum side up and the donor compartment dry and open to atmosphere. The membranes were then floated on the receiver solution for 12 h for equilibration and pre-hydration, to maintain a transepidermal hydration gradient. The receiver solution was then replaced with fresh medium. Test formulations (100 μl in a non-occluded open application) were applied to the skin surfaces, each having an available diffusion area of 2.01 cm^2, and were allowed to dry. DT solution (0.3%, w/v) in 30% (v/v) aqueous ethanol was used as a control. Aliquots (2 ml) of the receptor solution were removed at 2-h intervals for ultra-performance liquid chromatography–mass spectrometry (UPLC–MS) assay and were immediately replaced with fresh medium.

At the end of permeation experiments (12 h), the donor compartment and the skin surface were washed 5 times with receptor medium. The DT in the skin was extracted by incubation with 95% (v/v) aqueous methanol for 2 h. The DT concentration of the extraction solution was assayed by UPLC–MS, with resulting values used to calculate skin deposition.

The receptor medium was maintained at 37 ± 1 °C throughout experiments, to maintain the skin surface temperature at 32 °C. Each vesicular system was tested in 5 individual diffusion cells.

2.7. Tumor inhibition experiments in vivo

Experiments were performed at the Experimental Animal Center of the Zhejiang Academy of Medical Sciences under the institutional guidelines for the care and use of laboratory animals (Ethics Certificate No. 2014001812184). Male hairless mice (HRS/J) (4 w old, 42 mice), weighing 18–20 g, were subcutaneously injected with 0.2 ml A-375 human melanoma cells (8×10^9/l) in the armpit of their left forelimb. Mice were then housed individually in plastic cages in an air-conditioned room (22 ± 2 °C, 55 ± 5% humidity) and maintained on a 12-h light/12-h dark cycle with free access to food and water. After 14 d, all mice had tumors, with a median tumor volume of 203 mm^3. The mice were randomly divided into seven groups, labeled A–G. Group A was the control group and was maintained on the normal feeding schedule over the course of treatment of the other groups. The other groups were treated with: B, basic-nanoethosomes; C, EGCG-nanoethosomes (containing 0.2% EGCG); D, 0.3% DT in 30% aqueous ethanol; E, DT-EGCG-nanoethosomes (containing 0.2% EGCG + 0.3% DT); F, 0.2% EGCG + 0.3% DT in 30% aqueous ethanol; and G, DT-basic-nanoethosomes (containing 0.3% DT). All treatments were administered topically to the skin over the tumors. Each administered dose of DT was approximately 30 mg/kg. To treat topically, 180–200 μl of the sample solution on an adhesive bandage (1.5 cm × 1.5 cm) was attached to the skin over the tumor for 24 h and, every 3 d, a fresh bandage with the corresponding treatment sample was applied. Tumor size was measured at 2-d intervals. Tumor volume was calculated using the formula: tumor volume (mm^3) = ($W^2 \times L$)/2, where W is the width and L the length (in mm) of the tumor. At 2 d after the fifth dermal administration of drugs, the mice were sacrificed by cervical dislocation and the tumors were harvested, photographed and weighed.

2.8. Pharmacokinetics study

At 14 d after cells were subcutaneously implanted, when all mice had developed tumors giving a group median of 200 mm^3, mice were pair-matched according to their tumor volumes and, accordingly, divided into two groups. One group received 10 mg/kg DT by a single tail vein injection of DT solution (0.5 mg/ml) administered at 10 μl per gram body weight. The other group received 30 mg/kg DT by transdermal delivery using DT-EGCG-nanoethosomes, topically administering 10 μl solution per gram body weight. Mice (N = 6 per time point) were sacrificed at 0.083, 2, 4, 24 and 72 h after dosing. Blood (approximately 1 ml) was collected *via* terminal cardiac puncture using K3-EDTA as an anticoagulant under CO_2 anesthesia and plasma prepared by centrifugation (1500 × *g* for 5 min). Plasma and tissues were placed in cryopreservation vials, snap frozen in liquid nitrogen and stored at −80 °C until analysis. Tissues were homogenized in water (1:3, tissue:water) prior to analysis (Chu et al., 2013).

2.9. DT extraction and determination

DT stock solutions (1 mg/ml) were stored in methanol at −20 °C. The concentrations of DT in matrix (definition follows) used for standard curves were 1, 3, 5, 10, 30, 50, 100, 300, 500, 1000 and 3000 ng/ml and the concentrations used for quality control (QC) were 3, 30, 300 and 3000 ng/ml. The matrix for the standard curve and QC samples consisted of control mouse plasma for analysis of all plasma samples or control plasma mixed 1:1 with a control tissue homogenate for all tissue sample analyses. A liver/plasma surrogate matrix was used for analysis of tumor samples. All tumor and tissue homogenates were diluted 1:1 (v/v) with control plasma prior to analysis.

Samples were vortexed for 5 min and centrifuged at 3000 × *g* for 10 min at 4 °C. An aliquot (170 μl) of each supernatant was transferred to a clean 1.5-ml tube, lyophilized under nitrogen and dissolved in 60 μl MeOH/0.1% formic acid. Aliquots (50 μl) if these samples were transferred to a silanized glass 96-well plate insert containing 50 μl ddH_2O and 10 μl of each sample injected for LC–MS/MS analysis.

DT measurements were as described by Du et al. (2013). Chromatographic separation was performed on an ACQUITY UPLC system equipped with a BEH C_{18} column (50 mm × 2.1-mm i.d., 1.7-μm particle size; Waters Corp., Milford, MA, USA). The gradient

elution mobile phase was composed of 0.5% formic acid in water (A, pH 2.23) and 0.5% formic acid in acetonitrile (B, pH 2.24) delivered at a flow rate of 0.3 ml/min. The gradient was controlled as follows: 0–0.9 min, 90% A; 0.9–1.6 min, 100% B; 1.6–1.7 min, 90% A; 1.7–2.5 min, 90% A. The temperature of the column was maintained at 35 °C and the autosampler at 40 °C. For each analysis, an aliquot of 5.0 μ1 was injected into the UPLC–MS/MS system. Mass spectrometric analysis was performed on a QTRAP 5500 mass spectrometer (AB Sciex, Framingham, MA, USA) equipped with an electrospray ionization (ESI) source in the positive ionization mode with ion spray voltage at 4500 V, turbo-gas temperature at 400 °C, curtain gas at 40.0 psi and ion source Gas 1 (nebulizer) at 40.0 psi and turbo ion source Gas 2 (heater) at 35.0 psi. The declustering potential and entrance potential were set at 110 V and 10 V, respectively. A collision energy of 18.0 eV and collision cell exit potential of 13.0 V were utilized. The DT scans were optimized by the proton adduct $[M+H]^+$ ion and the MRM transitions were at *m/z* 808.3 and 527.1. Data acquisition and peak integration were performed using Analyst software (version 1.5.1, AB Sciex).

2.10. Statistical and pharmacokinetics analysis

The Student's *t*-test was used when only two groups were compared. One way analysis of variance (ANOVA) followed by a modified *t*-test for multiple comparisons was used when more than two groups were compared. Pharmacokinetics data were analyzed by noncompartmental methods using Winnonlin Professional Edition version 5.2 (Pharsight Corp, Cary, NC, USA). The area under the concentration *versus* time curve from 0 to t (AUC_{0-t}) was calculated using the linear up/log down rule. Volume of distribution (V_d) and clearance (CL) were calculated using standard equations. The maximum concentration (C_{max}) and time of C_{max} (T_{max}) were determined by visual inspection of the concentration *versus* time curve data.

3. Results and discussion

3.1. Characterization of EGCG-nanoethosomes

Nanoethosomes were prepared under various conditions to achieve a stable and bioavailable suspension. Experiments covered single and multiple factors related to the composition. Basic-nanoethosomes (Fig. 1A) with a mean diameter of 71.3 ± 4.9 nm and a ZP of −30.4 ± 1.2 mV (Table 1) were prepared with 2% soybean phosphatidylcholine (SPC, Lipoid S100), 30% ethanol, 1% Tween-80 and 0.1% sugar esters by a modification of the method described by Touitou et al. (2000). Nanosuspensions with a ZP above 30 mV or below −30 mV are normally regarded as stable (Stevanovic et al., 2012), and a mean diameter from 50 to 70 nm is considered to be the optimal nanoparticle size range for uptake into cells (Chithrani et al., 2006). When 0.2% EGCG (w/w) was loaded into the basic-nanoethosomes, EGCG-nanoethosomes were obtained with a mean diameter of 60.5 ± 3.5 nm (Fig. 1B) and a ZP of −43.5 ± 2.9 mV (Table 1), a more stable potential and constant diameter than the basic-nanoethosomes.

Table 1
Characteristics of basic-nanoethosomes and EGCG-nanoethosomes.

Feature	Basic-nanoethosomes	EGCG-nanoethosomes
Mean diameter (nm)	71.3 ± 4.9 [a]	60.5 ± 3.5 [b]
Zeta potential (mV)	−30.4 ± 1.2 [a]	−43.5 ± 2.9 [b]
Polydispersity index	0.089 ± 0.010 [a]	0.087 ± 0.012 [a]

All values are means ± SD (n = 3). [a,b]Different letters in the same line indicate significant differences among mean values ($p < 0.05$).

It was interesting to note that EGCG-nanoethosomes were smoother and had a more compact structure than basic-nanoethosomes, which led us to investigate the transdermal permeability of EGCG-nanoethosomes, compared with basic-nanoethosomes.

3.2. Transdermal permeability of EGCG-nanoethosomes in vitro

The transdermal permeability of EGCG-nanoethosomes and basic-nanoethosomes *in vitro* was determined by evaluating their skin penetration by confocal laser scanning microscopy. To allow imaging, nanoethosomes were combined with the fluorescent probe rhodamine red. Fig. 2 shows the residual amount of basic-nanoethosomes and EGCG-nanoethosomes at different skin depths from 10 to 150 μm. The basic-nanoethosomes with red fluorescence were primarily located in the epidermis and dermis (10–50 μm) (Fig. 2A) while EGCG-nanoethosomes penetrated through the epidermis and dermis and were primarily located in the hypodermis (60–150 μm), as shown by the net structure of the hypodermis with red fluorescence (Fig. 2B). These results indicated that EGCG-nanoethosomes had greater transdermal permeability than basic-nanoethosomes. This advantage of EGCG-nanoethosomes may make them useful as carriers for transdermal delivery of bioactive components.

3.3. EGCG-nanoethosomes as DT carriers

To demonstrate that the EGCG-nanoethosome was a better carrier than the basic-nanoethosome for transdermal delivery of bioactive substances, DT-EGCG-nanoethosomes and DT-basic-

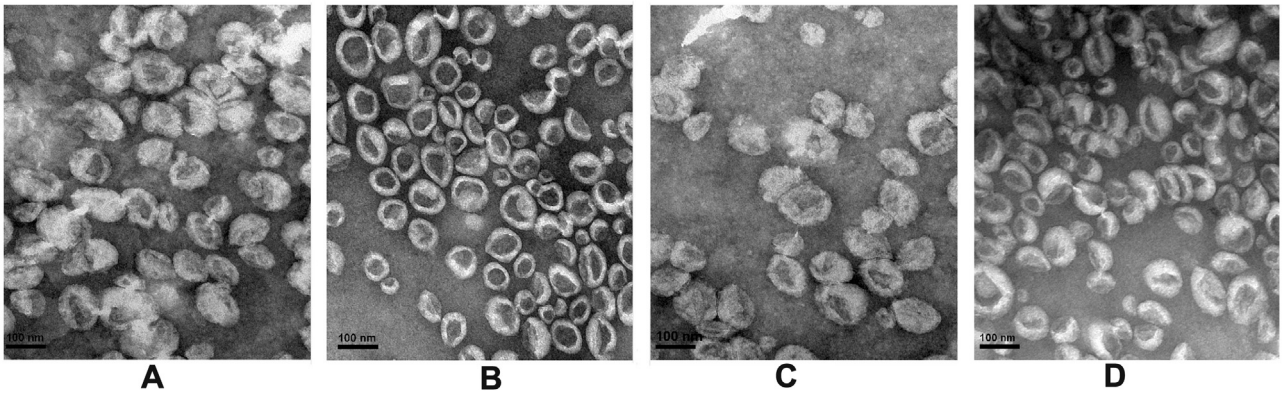

Fig. 1. Transmission electron microscopic images of basic- and EGCG-nanoethosomes loaded with/without DT. (A) Basic-nanoethosomes, (B) EGCG-nanoethosomes, (C) DT-baisc-nanoethosomes, (D) DT-EGCG-nanoethosomes. Bar = 100 μm.

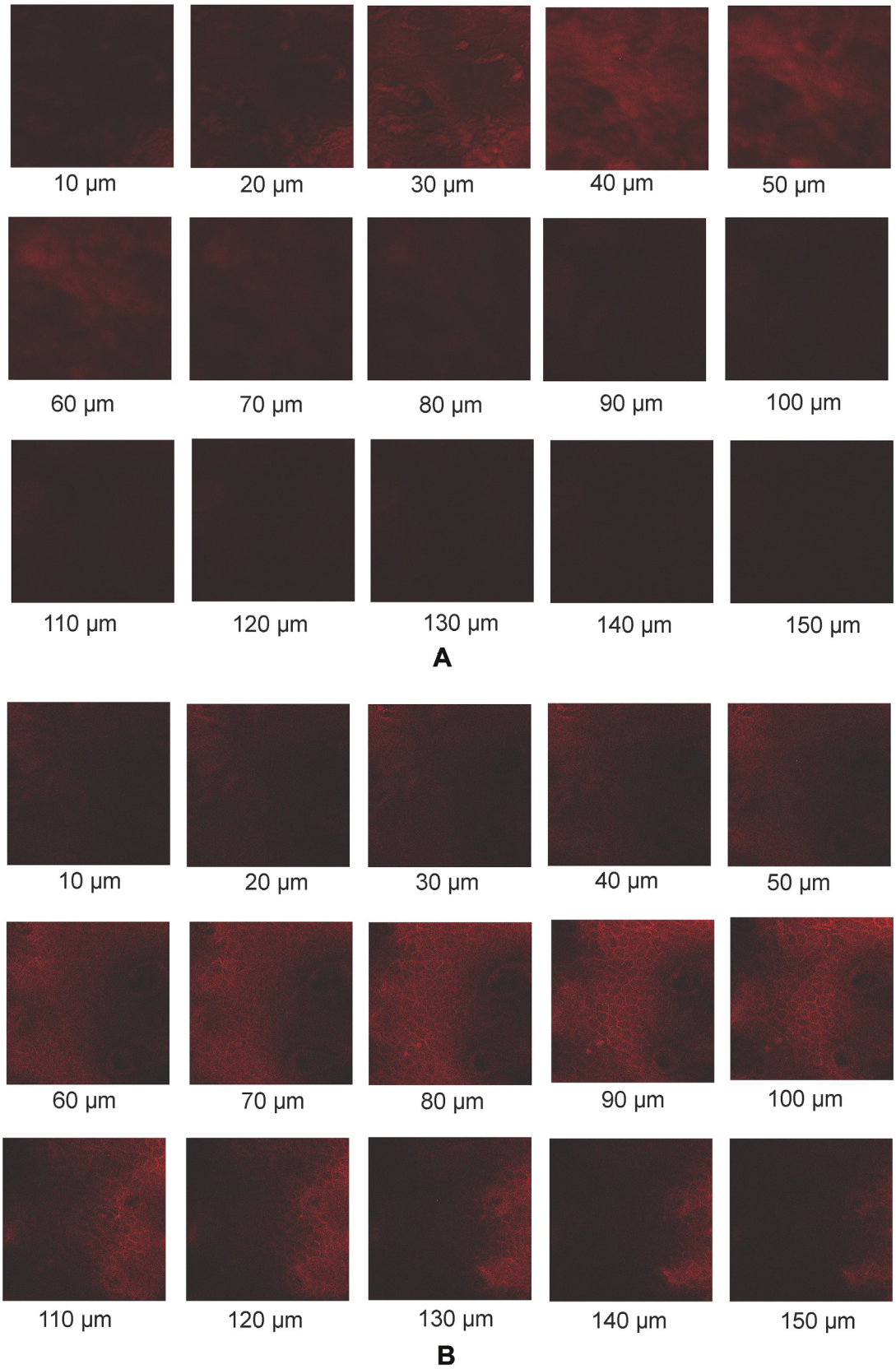

Fig. 2. Visual observation of the penetration of nanoethosomes through skin by confocal laser scanning microscopy. (A) Basic-nanoethosomes, (B) EGCG-nanoethosomes. Bar = 20 μm.

nanoethosomes were prepared for testing in anti-tumor experiments. The DT-EGCG-nanoethosomes with a DT loading of 0.3% had a mean diameter of 72.4 ± 4.5 nm (Fig. 1D) and a ZP of −29.1 ± 1.4 mV, similar in morphology and size to EGCG-nanoethosomes (Fig. 1B). Their morphology differed from that of the DT-basic-nanoethosomes, which had a mean diameter of 62.1 ± 3.6 nm (Fig. 1C) and a ZP of −41.1 ± 2.2 mV, similar to those of basic-nanoethosomes (Fig. 1A). The DT-EGCG-nanoethosomes were smoother and more compact than DT-basic nanoethosomes, results similar to the comparison between EGCG-nanoethosomes and basic-nanoethosomes.

3.4. Stability of EGCG-nanoethosomes

The stability of EGCG-nanoethosomes was determined by examining the changes of size and zeta potential at 4–8 °C, with results shown in Table 2. The sizes of the basic-nanoethosomes and EGCG-nanoethosomes were slightly increased after 180 d storage. The increased size of EGCG-nanoethosomes was positively correlated to their EGCG leakage rate. We inferred that the EGCG was gradually lost during storage because of its oxidation, causing an increase in the size of the EGCG-nanoethosomes. However, the stability of the EGCG-nanoethosomes was higher than that of basic-nanoethosomes because their ZP was still less than −30 mV after 90 d storage.

The changes in mean diameter and ZP of the DT-EGCG-nanoethosomes were similar to those of the EGCG-nanoethosomes under the same storage conditions (Table 3). We found a very low DT leakage from the DT-EGCG-nanoethosomes, which was likely related to the low polarity of DT because SPC and ethanol are the major constituents of nanoethosomes. Therefore, stability of DT-EGCG-nanoethosomes primarily reflected the satisfactory stability of EGCG-nanoethosomes.

3.5. In vitro *permeation and skin deposition*

To understand the beneficial effects of the DT-EGCG-nanoethosomes in delivering DT we investigated the *in vitro* skin permeation and deposition of DT released by DT-EGCG-nanoethosomes. Fig. 3A shows DT permeation through mouse skin *in vitro* from an application of a DT-EGCG-nanoethosome suspension (NTS method). The cumulative permeation of DT delivered by the NTS method was significantly higher than that delivered by application of a DT-aqueous 30% ethanol solution (AES method).

Table 2
Changes in mean diameter, zeta potential and EGCG leakage rate of EGCG-nanoethosomes.

Storage time (days)	Basic-nanoethosomes		EGCG-nanoethosomes		
	Diameter (nm)	Zeta potential (mV)	Diameter (nm)	Zeta potential (mV)	EGCG leakage rate (%)
0	71.5 ± 4.2 [a]	−30.6 ± 1.1 [a]	60.8 ± 3.3 [a]	−43.5 ± 2.9 [a]	0
30	71.1 ± 3.8 [a]	−30.4 ± 1.0 [a]	62.8 ± 4.3 [ab]	−42.5 ± 3.6 [a]	4.1 ± 0.6 [a]
60	72.5 ± 4.4 [a]	−29.8 ± 1.3 [a]	63.3 ± 3.8 [ab]	−39.5 ± 2.3 [b]	7.4 ± 1.0 [b]
90	74.5 ± 4.1 [a]	−28.0 ± 1.6 [b]	66.6 ± 4.4 [b]	−33.5 ± 1.9 [c]	14.3 ± 1.5 [c]

All values are means ± SD (n = 3). [a,b,c] Different letters in the same column indicate significant differences among mean values ($p < 0.05$).

Table 3
Changes in mean diameter, zeta potential and DT leakage rate of DT-EGCG-nanoethosomes during storage at 4–8 °C.

Storage time (days)	Diameter (nm)	Zeta potential (mV)	DT leakage rate (%)
0	62.1 ± 3.6 [a]	−41.1 ± 2.2 [a]	0
30	62.4 ± 4.0 [a]	−40.5 ± 3.6 [a]	0.11 ± 0.01 [a]
60	63.1 ± 3.3 [a]	−39.1 ± 2.1 [a]	0.14 ± 0.02 [b]
90	65.8 ± 4.9 [a]	−32.2 ± 1.6 [b]	0.17 ± 0.05 [c]

All values are means ± SD (n = 3). [a,b,c] Different letters in the same column indicate significant differences among mean values ($p < 0.05$).

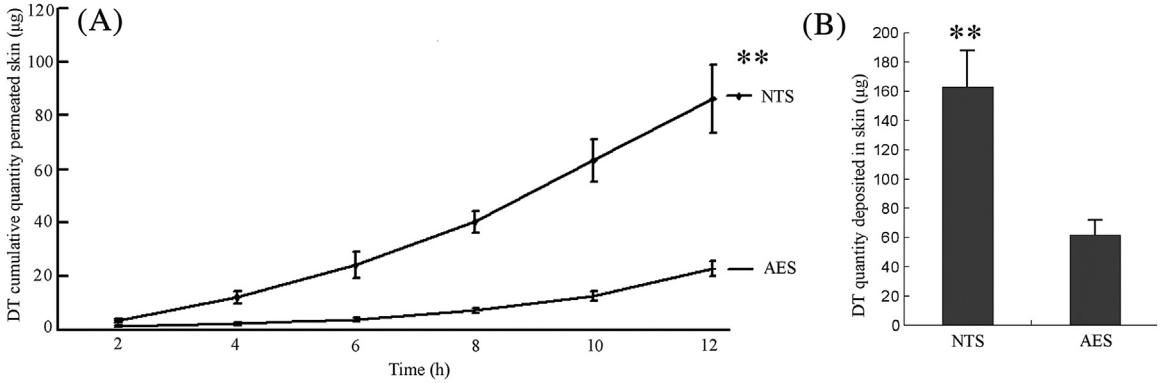

Fig. 3. DT permeation and deposition against mice skin *in vitro* from 100 μl DT-EGCG-nanoethosomes suspension (NTS) and 100 μl DT-aqueous 30% ethanol solution (AES). (A) Cumulative DT that permeated the skin. (B) Skin deposited DT after 12 h of application of drugs. Data are expressed as mean ± SEM (n = 5). $^{**}P < 0.01$, data of NTS compared to data of AES.

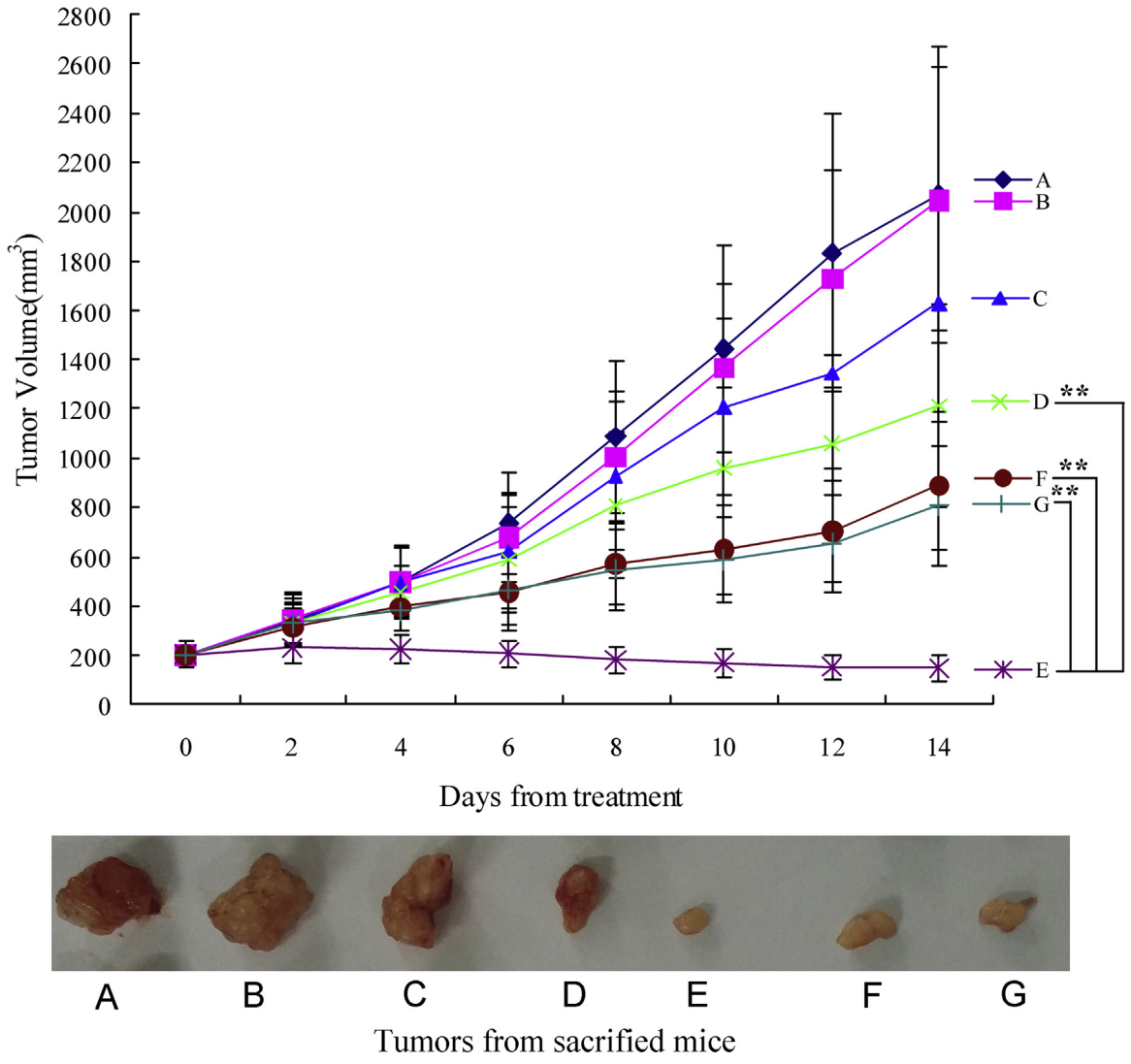

Fig. 4. The effectiveness of DT-EGCG-nanoethosomes on inhibiting the growth of human melanoma tumors of mice from inoculated A-375 human melanoma cells. (A) tumors without sample treatment, (B) tumors treated with basic-nanoethosome formulation, (C) tumors treated with EGCG-nanoethosome formulation (0.2% EGCG), (D) tumors treated with 0.3% DT in 30% aqueous ethanol, (E) tumors treated with DT-EGCG-nanoethosome formulation (containing 0.2% EGCG + 0.3% DT), (F) tumor treated with 0.2% EGCG + 0.3% DT in 30% aqueous ethanol, (G) tumors treated with DT-basic-nanoethosome formulation (containing 0.3% DT). Tumors were obtained two day later after the last sample treatment. ** $P < 0.01$.

The cumulative permeation of DT over 12 h for the NTS method was 27.8% (mean) of the dosage (300 μg) while the AES method gave only 7.3% permeation. The deposition of DT in the skin (Fig. 3B) after 12 h treatment by the NTS method was 54.3% of the dosage while the AES method led to deposition of only 20.6% of the dosage. Clearly, EGCG-nanoethosomes can facilitate DT permeation through the skin and its release at target locations under the skin, such as a tumor.

3.6. Tumor growth inhibition

Fig. 4 shows the effectiveness of DT-EGCG-nanoethosomes at inhibiting human melanoma tumor growth in mice implanted subcutaneously with A-375 human melanoma cells. There was little difference in tumor volumes in the control group (A) and the basic-nanoethosome treated group (B), demonstrating that basic-nanoethosomes did not influence tumor growth. However, in mice treated with EGCG-nanoethosomes (C) tumor growth was inhibited by 21.4% compared with the control group ($p < 0.05$), suggesting that EGCG showed anti-cancer activity. Treatment with DT-EGCG-nanoethosomes (containing 0.2% EGCG + 0.3% DT) (E) inhibited tumor growth by 92.9% ($p < 0.01$), while treatments with 0.3% DT (D), 0.2% EGCG + 0.3% DT (F) and DT-basic-nanoethosomes (containing 0.3% DT) (G) caused tumor inhibition rates of 41.4%, 57.0% and 61.0% respectively, compared with the control group. Of all the groups only the group treated with DT-EGCG-nanoethosomes exhibited a significant therapeutic effect with tumor volume decreased 31.5% after 14 d treatment. In contrast, the groups treated with 0.3% DT, 0.2% EGCG + 0.3% DT or DT-basic-nanoethosomes showed no therapeutic effects.

Based on the tumor weights, treatment with DT-EGCG-nanoethosomes significantly inhibited tumor growth by 92.2%, while treatments with 0.3% DT, 0.2% EGCG + 0.3% DT and DT-basic-nanoethosomes (containing 0.3% DT) resulted in tumor inhibition rates of 48.8%, 72.3% and 73.2%, respectively (Table 4). These results were consistent with those based on tumor volumes.

Table 4
Mean tumor weights and percent tumor inhibition rates in tumor-bearing mice after various treatments.

Group	Treatment	Tumor weight (g)	Tumor inhibition compared with group A (%)
A	/	1.695 ± 0.391^{a}	/
B	Basic-nanoethosomes	1.677 ± 0.342^{a}	1.3
C	EGCG-nanoethosomes	1.264 ± 0.266^{ab}	25.4
D	DT	0.867 ± 0.241^{b}	48.8
E	DT-EGCG-nanoethosomes	0.132 ± 0.046^{c}	92.2
F	DT +EGCG	0.469 ± 0.142^{d}	72.3
G	DT-basic-nanoethosomes	0.455 ± 0.129^{d}	73.2

Data are means (±SD) of six replicates. ^{a,b,c,d} Different letters in the same column indicate significant differences among mean values ($p < 0.05$). (−)-Epigallocatechin-3-*O*-gallate (EGCG), Docetaxel (DT).

A high concentration of drug at the site of action is necessary for its therapeutic activity. If the concentration of drug does not reach a minimum cytotoxic level, no appreciable therapeutic response will be achieved, as we observed with 0.2% EGCG + 0.3% DT, 0.3% DT and DT-basic-nanoethosomes treatments in our study. We encountered this problem with DT-EGCG-nanoethosomes for dermal administration, which should have produced high DT concentrations in the tumor tissues. Moreover, EGCG has shown anticancer, anti-HIV, neuroprotective and DNA-protective effects (Nagle et al., 2006). Though many studies have described beneficial bioactivities of EGCG, here we have utilized EGCG to improve permeation of drug loaded into nanoethosomes through the skin.

It should be mentioned that a very low DT leakage from the DT-EGCG-nanoethosomes was found during storage at 4–8 °C. But DT release from DT-EGCG-nanoethosomes *in vivo* became fast. This indicates that the nanoethosomes were influenced by the *in vivo* environment. The pH of the DT-EGCG-nanoethosomes suspension showed a value of 6.94 while pH of the body fluid is 7.2-7.4. As we know, EGCG was very un-stable at body fluid due to the meta-alkaline environment (Lambert et al., 2002; Krook and Hagerman, 2012). When DT-EGCG-nanoethosomes reached the subcutaneous tissue the nanoethosomes was disintegrated due to the degradation of EGCG under meta-alkaline environment to release. Moreover, the disassembly of DT could be accelerated by the body temperature, which also might cause the DT release from the nanoethosomes.

3.7. Pharmacokinetics

Because transdermal delivery is slower and less efficient than intravenous injection, the DT dose we used in our experiments for intravenous administration was 10 mg/kg while that for dermal administration was equivalent to 30 mg/kg. Mean concentration-time curves of DT in mouse plasma and tissues after intravenous administration of free DT or topical dermal administration of DT-EGCG-nanoethosomes are shown in Fig. 5. We observed that transdermal delivery using DT-EGCG-nanoethosomes showed advantageous sustained release properties. That is, intravenous administration produced DT concentrations greater than 2000 ng/l for only 8 h while the dermal administration yielded these DT levels for 36 h. Moreover, the dermal administration decreased cytoxicity of DT to the liver, lung and spleen because the maximum concentrations of DT by dermal administration were much lower than those by intravenous administration.

The major pharmacokinetic parameters of DT after intravenous drug injection and topical dermal administration with DT-EGCG-nanoethosomes are shown in Table 5. DT tumor exposure, as measured by AUC of the concentration-time curve, was 2.48-fold higher in mice receiving 30 mg/kg by topically administered DT-EGCG-nanoethosomes compared with 10 mg/kg DT by tail vein injection. The time of maximum concentration (T_{max}) for tumors was 24 h, consistent with the *in vitro* skin permeation and deposition of DT (Fig. 3). The mean residence time (MRT) of DT in tumors was 4.58-fold higher for mice receiving 30 mg/kg by topical DT-EGCG-nanoethosomes than for those receiving 10 mg/kg DT intravenously. These results demonstrated that the transdermal delivery by DT-EGCG-nanoethosomes was efficient for exposure of the tumor to DT.

Transdermal drug delivery is an attractive alternative to oral delivery because it can minimize first-pass effects, avoid gastrointestinal irritation and improve patient compliance (Lu et al., 2002). Moreover, transdermal delivery can provide a prolonged and constant systemic absorption profile, potentially reducing several side effects caused by fluctuating plasma drug concentrations (Prausnitz and Lauger, 2008; Kamran et al., 2016). In our study EGCG-nanoethosomes were used, for the first time, to improve transdermal drug delivery. Our strategy may promote further development of nanoethosome technology to achieve wider applications for transdermal drug delivery in the pharmaceutical and cosmetics industries. Moreover, EGCG, the major and most physiologically bioactive compound found in tea leaves, was shown to prevent oxidative injuries and depletion of antioxidant enzymes in animal and human skin exposed to UVB rays (Wang et al., 1991) and to have benefits for treating cancers and cardiovascular disease (Singh et al., 2011; Yang et al., 2009; Widlansky et al., 2007). Therefore, the bioactivities of EGCG itself can also be utilized as EGCG-nanoethosomes are applied as drug carriers.

Nanosuspension technologies have been studied extensively in recent years. However, their applications in the pharmaceutical and nutraceutical industries have been limited, primarily because of stability concerns (Sudhakar et al., 2014). In our study EGCG was used, for the first time, to improve skin penetration of nanoethosome suspensions. This strategy may lead to further development of nanoethosome technologies to increase their applications for transdermal drug delivery in the pharmaceutical and cosmetic industries.

4. Conclusion

EGCG-nanoethosomes composed of 0.2% EGCG, 2% soybean phosphatidylcholine, 30% ethanol, 1% Tween-80 and 0.1% sugar esters were prepared. These nanoethosomes were smoother and more compact than basic-nanoethosomes with the same components except for EGCG. The improved transdermal delivery properties of EGCG-nanoethosomes, compared with basic-nanoethosomes, were elucidated using an *in vitro* mouse skin permeation test. EGCG-nanoethosomes loaded with DT (DT-

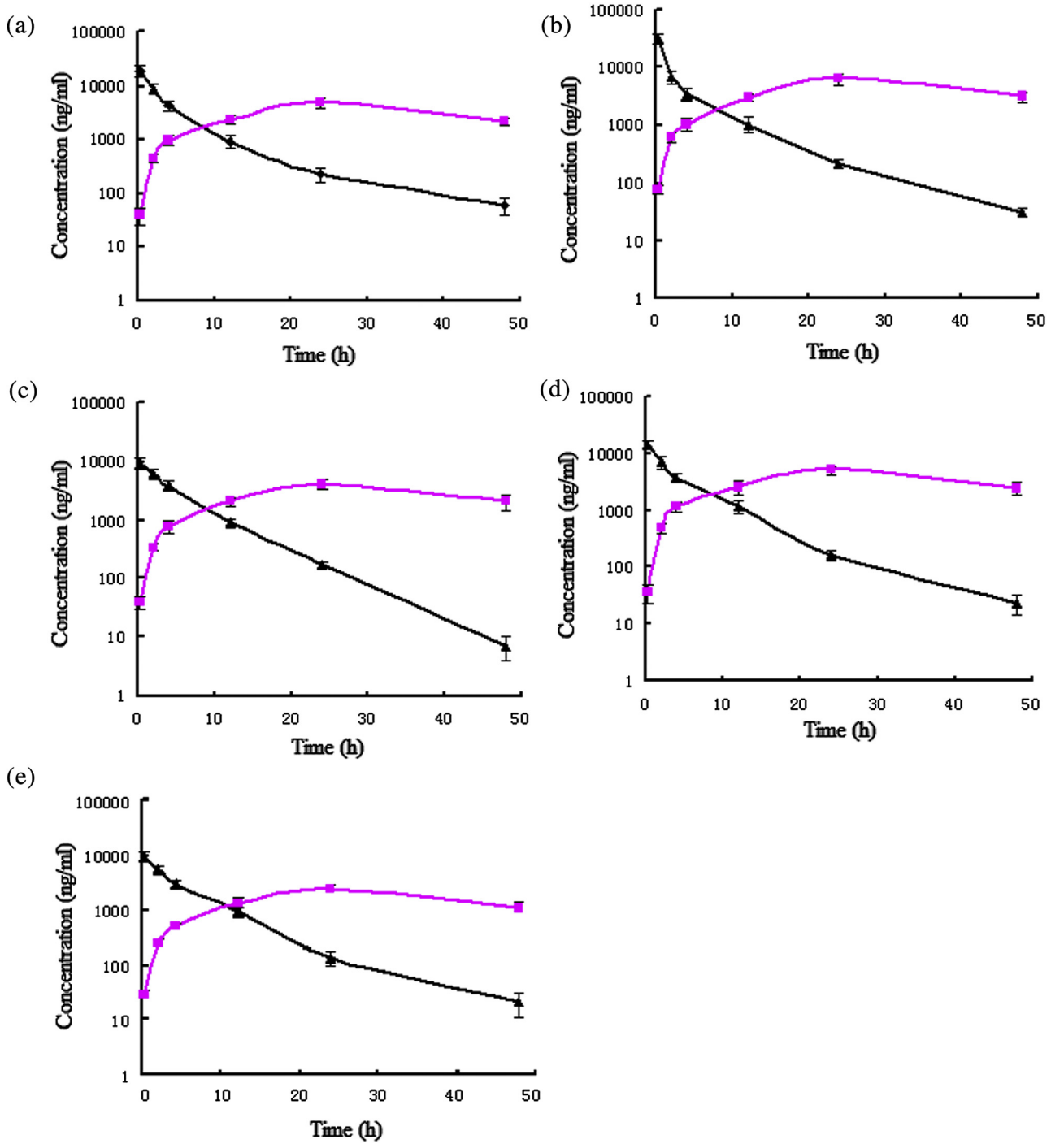

Fig. 5. Pharmacokinetic profiles of DT in (A) Plasma, (B) Tumor, (C) Liver, (D) Spleen and (E) Lung. Square: intravenous administration of free DT injection (10 mg/kg), Triangle: topical dermal administration by DT-EGCG-nanoethosomes (30 mg/kg of equivalent DT).

EGCG-nanoethosomes) showed excellent transdermal delivery of DT and inhibited growth of A-375 human melanoma cell tumors implanted into mice. The group treated with DT-EGCG-nanoethosomes exhibited a significant therapeutic effect, with tumors shrinking to 31.5% of their initial volumes after 14 d treatment. This suggested that DT-EGCG-nanoethosomes have potential value for treating skin cancer. Taken together, our results demonstrated that EGCG-nanoethosomes are very promising as carriers for transdermal drug delivery.

Acknowledgments

This research was supported by the Fund for Distinguished Scholars of Zhejiang Agricultural and Forestry University (2014FR064), and grants from the National Natural Science Foundation of China (Grant 31270724), the National Key Technology R&D Program (2012BAD36B06) and the Natural Science Foundation of Zhejiang Province (Grant LZ12C16004).

Table 5
Major pharmacokinetic parameters of DT after intravenous DT injection (10 mg/kg) or topical dermal administration of DT-EGCG-nanoethosomes (30 mg/kg of equivalent DT) (means ± SD; n = 6).

Specimen	Parameter	Formulation	
		DT *via* vein	DT-EGCG-nanoethosomes *via* skin
Plasma	AUC (μg/l h)	65,837 ± 14,148	135,935 ± 26,006
	C_{max} (μg/l)	NA[a]	4707 ± 991
	T_{max} (h)	NA	24.0 ± 0.0
	MRT_{0-t} (h)	5.74 ± 0.30	27.1 ± 0.3
	Vd (L/kg)	2118 ± 457	NA
	$T_{1/2}$	9.43 ± 0.43	NA
	CL (L/h/kg)	0.157 ± 0.037	NA
Tumor	AUC (μg/l h)	48,664 ± 9084	120,792 ± 24,637
	T_{max} (h)	NA	24.0 ± 0.0
	C_{max} (μg/l)	NA	4081 ± 735
	MRT_{0-t} (h)	5.85 ± 0.05	27.4 ± 0.4
Liver	AUC (μg/l h)	71,053 ± 16,010	187,907 ± 36,552
	T_{max} (h)	NA	24.0 ± 0.0
	C_{max} (μg/l)	NA/	6814 ± 1513
	MRT_{0-t} (h)	4.93 ± 0.07	27.5 ± 0.2
Spleen	AUC (μg/l h)	43,979 ± 7985	152,899 ± 32,500
	T_{max} (h)	NA	24.0 ± 0.0
	C_{max} (μg/l)	NA	2533 ± 495
	MRT_{0-t} (h)	6.09 ± 0.24	26.9 ± 0.2
Lung	AUC (μg/l h)	579,671 ± 2816	72,594 ± 16,016
	T_{max} (h)	NA	24.0 ± 0.0
	C_{max} (μg/l)	NA	5231 ± 912
	MRT_{0-t} (h)	5.78 ± 0.09	27.1 ± 0.2

[a] Unavailable for determination.

References

Chandel, A., Patil, V., Goyal, R., Dhamija, H., Parashar, B., 2012. Ethosomes: a novel approach towards transdermal drug delivery. Int. J. Pharm. Chem. Sci. 1, 563–569.

Chithrani, B.D., Ghazani, A.A., Chan, W.C.W., 2006. Determining the size and shape dependence of gold nanoparticle uptake into mammalian cells. Nano Lett. 6, 662–668.

Chu, K.S., Schorzman, A.N., Finniss, M.C., Bowerman, C.J., Peng, L., Luft, J.C., Madden, A.J., Wang, A.Z., Zamboni, W.C., DeSimone, J.M., 2013. Nanoparticle drug loading as a design parameter to improve docetaxel pharmacokinetics and emcacy. Biomaterials 34, 8424–8429.

Clarke, S.J., Rivory, L.P., 1999. Clinical pharmacokinetics of docetaxel. Clin. Pharmacokinet. 36, 99–114.

D'Orazio, J., Jarrett, S., Amaro-Ortiz, A., Scott, T., 2013. UV radiation and the skin. Int. J. Mol. Sci. 14, 12222–12248.

Du, P., Li, N., Wang, H., Yang, S., Song, Y., Han, X., Shi, Y., 2013. Development and validation of a rapid and sensitive UPLC-MS/MS method for determination of total docetaxel from a lipid microsphere formulation in human plasma. J. Chromatogr. B 926, 101–107.

Dubey, V., Mishra, D., Dutta, T., Nahar, M., Saraf, D.K., Jain, N.K., 2007a. Dermal and transdermal delivery of an anti-psoriatic agent via ethanolic liposomes. J. Control. Release 123, 148–154.

Dubey, V., Mishra, D., Jain, N.K., 2007b. Melatonin loaded ethanolic liposomes: physicochemical characterization and enhanced transdermal delivery. Eur. J. Pharm. Biopharm. 67, 398–405.

Elsayed, M.M.A., Abdallah, O.Y., Naggar, V.F., Khalafallah, N.M., 2006. Lipids vesicles for skin delivery of drugs: reviewing three decades of research. Int. J. Pharm. 332, 1–16.

Hong, Z., Xu, Y., Yin, J., Jin, J., Jiang, Y., Du, Q., 2014. Improving the effectiveness of (−)-epigallocatechin gallate (EGCG) against rabbit atherosclerosis by EGCG-loaded nanoparticles prepared from chitosan and polyaspartic acid. J. Agric. Food Chem. 62, 12603–12609.

Kamran, M., Ahad, A., Aqil, M., Imam, S.S., Sultana, Y., Ali, A., 2016. Design, formulation and optimization of novel soft nano-carriers for transdermal olmesartan medoxomil delivery: *in vitro* characterization and in vivo pharmacokinetic assessment. Int. J. Pharm. 505, 147–158.

Krook, M.A., Hagerman, A.E., 2012. Stability of polyphenols epigallocatechin gallate and pentagalloyl glucose in a simulated digestive system. Food Res. Int. 49, 112–116.

Lambert, J.D., Lee, M.J., Diamond, L., Ju, J., Hong, J., Bose, M., Newmark, H.L., Yang, C. S., 2002. Pharmacokinetics of tea catechins after ingestion of green tea and (−)-epigallocatechin-3-gallate by humans: formation of different metabolites and individual variability. Cancer Epidemiol. Biomarkers Prev. 11, 1025–1032.

Lambert, J.D., Lee, M.J., Diamond, L., Ju, J., Hong, J., Bose, M., Newmark, H.L., Yang, C. S., 2006. Dose-dependent levels of epigallocatechin-3-gallate in human colon cancer cells and mouse plasma and tissues. Drug Metab. Dispos. 34, 8–11.

Lee, E.Y., Chun, M.K., Chang, J.S., Choi, H.K., 2014. Development of matrix based transdermal delivery system for ketotifen. J. Pharm. Invest. 44, 291–296.

Li, N., Taylor, L.S., Ferruzzi, M.G., Mauer, L.J., 2013. Color and chemical stability of tea polyphenol (−)-epigallocatechin-3-gallate in solution and solid states. Food Res. Int. 53, 909–921.

Lu, Y.P., Lou, Y.R., Xie, J.G., Peng, Q.Y., Liao, J., Yang, C.S., Huang, M.T., Conney, A.H., 2002. Topical applications of caffeine or (−)-epigallocatechin gallate (EGCG): inhibit carcinogenesis and selectively increase apoptosis in UVB-induced skin tumors in mice. Proc. Natl. Acad. Sci. U. S. A. 99, 12455–12460.

Madheswaran, T., BasKaran, R., Yong, C.S., Yoo, B.K., 2014. Enhanced topical delivery of finasteride using glyceryl monooleate-based liquid crystalline nanoparticles stabilized by cremophor surfactants. AAPS PharmSciTech 15, 44–51.

Nagle, D.G., Ferreira, D., Zhou, Y.D., 2006. Epigallocateehin·3-gallate (EGCG): chemical and biomedical perspectives. Phytochemistry 67, 1849–1855.

Narayanan, D.L., Saladi, R.N., Fox, J.L., 2010. Ultraviolet radiation and skin cancer. Int. J. Dermatol. 49, 978–986.

Prausnitz, M.R., Lauger, R., 2008. Transdermal drug delivery. Nat. Biotechnol. 26, 1261–1268.

Sang, S., Lee, M.J., Hou, Z., Ho, C.T., Yang, C.S., 2005. Stability of tea polyphenol (−)-epigallocatechin-3-gallate and formation of dimers and epimers under common experimental conditions. J. Agric. Food. Chem. 53, 9478–9484.

Simoes, M.C.F., Sousa, J.J.S., Pais, A.C.C., 2015. Skin cancer and new treatment perspectives: a review. Cancer Lett. 357, 8–42.

Singh, B.N., Shankar, S., Srivastava, R.K., 2011. Green tea catechin, epigallocatechin-3-gallate (EGCG): mechanisms, perspectives and clinical applications. Biochem. Pharmacol. 82, 1807–1821.

Stevanovic, M.M., Skapin, S.D., Bracko, I., Milenkovic, M., Petkovic, J., Filipic, M., Uskokovic, D.P., 2012. Poly(lactide-co-glycolide)/silver nanoparticles: synthesis, characterization, antimicrobial activity, cytotoxicity assessment and ROS-inducing potential. Polymer 53, 2818–2828.

Sudhakar, B., NagaJyothi, K., Murthy, K.V., 2014. Nanosuspensions as a versatile carrier based drug delivery system—an overview. Curr. Drug Deliv. 11, 299–305.

Touitou, E., Godin, B., 2007. Review: dermal drug delivery with ethosomes: therapeutic potential. Therapy 4, 465–472.

Touitou, E., Dayan, N., Bergelson, L., Godin, B., Eliaz, M., 2000. Ethosomes-novel vesicular carriers for enhanced delivery: characterization and skin penetration properties. J. Control. Release 65, 403–418.

Touitou, E., Godin, B., Dayan, N., Weiss, C., Piliponsky, A., Levi-Schaffer, F., 2001. Intracellular delivery mediated by an ethosomal carrier. Biomaterials 22, 3053–3059.

Verma, P., Pathak, K.J., 2010. Therapeutic and cosmeceutical potential of ethosomes: an overview. J. Adv. Pharm. Technol. Res. 1, 274–282.

WHO, 2011. Ultraviolet Radiation and the INTERSUN Programme-Skin CancersWorld Health Organization. . Available from: http://www.who.int/uv/faq/skincancer/en/indexl.html.

Wang, Z.Y., Agarwal, R., Bickers, D.R., Mukhtar, H., 1991. Protection against ultraviolet B radiation-induced photocarcinogenesis in hairless mice by green tea polyphenols. Carcinogensis 12, 1527–1530.

Wang, R., Zhou, W.B., Jiang, X.H., 2008. Reaction kinetics of degradation and epimerization of epigallocatechin gallate (EGCG): in aqueous system over a wide temperature range. J. Agric. Food Chem. 56, 2694–2701.

Warden, B.A., Smith, L.S., Beecher, G.R., Balentine, D.A., Clevidence, B.A., 2001. Catechins are bioavailable in men and women drinking black tea throughout the day. J. Nutr. 131, 1731–1737.

Widlansky, M.E., Hamburg, N.M., Anter, E., Holbrook, M., Kahn, D.F., Elliott, J.G., Keaney Jr., J.F., Vita, J.A., 2007. Acute EGCG supplementation reverses endothelial dysfunction in patients with coronary artery disease. J. Am. Coll. Nutr. 26, 95–102.

Xing, X.J., Yang, L., You, Y., Zhong, B.Y., Song, Q.H., Deng, J., Hao, F., 2011. Study of the biological function and penetration pathways of the mouse epidermal growth factor ethosomal delivery system. Exp. Dermatol. 20, 945–947.

Yang, C.S., Wang, X., Lu, G., Picinich, S.C., 2009. Cancer prevention by tea: animal studies, molecular mechanisms and human relevance. Nat. Rev. Cancer 9, 429–439.

Zaveri, N.T., 2006. Green tea and its polyphenolic catechins: medicinal uses in cancer and noncancer applications. Life Sci. 78, 2073–2080.

Zhang, Z., Wo, Y., Zhang, Y., Wang, D., He, R., Chen, H., Cu, D., 2012. *In Vitro* study of ethosome penetration in human skin and hypertrophic scar tissue. Nanomed. Nanotechnol. Biol. Med. 8, 1026–1033.